Secondary modulation instability of partially coherent beams in anisotropic media

Björn Gütlich, Cornelia Denz, Thomas König

Institut für Angewandte Physik, Westflische Wilhelms Universität Münster,
Corrensstrasse 2, 48149 Münster, Germany
phone: +49 (0)251-83-33517, fax: +49 (0)251-83-33513,
e-mail: guetlich@uni-muenster.de

Kristian Motzek, and Friedemann Kaiser

Institut für Angewandte Physik, Tehnische Universtiät Darmstadt,
Hochschulstrasse 4a, 64289 Darmstadt, Germany

Abstract: We experimentally and numerically investigate the modulation instability of incoherent optical beams in photorefractive media. Due to material anisotropy the modulation instability occurs successively from formation of stripes at a first threshold to full two dimensional filaments at a second threshold. We study the dependence of these onsets on the coherence properties of the beam. We derive experimental thresholds for modulation instability from contrast measurements and compare experimental and numerical results.

OCIS codes: (190.4420) Nonlinear optics, transverse effects in; (190.5330) Photorefractive nonlinear optics; (190.5530) Pulse propagation and solitons

The break up of optical beams into filaments in presence of a nonlinearity is a well known phenomenon [1–5]. Reason for the filamentation is the development of a modulation instability (MI), which means a noisy uniform solution becomes unstable against perturbations of a specific length or time scale and a self- organized solution with a scaling typical for the system evolves. Interest in modulation instability of optical beams arises from the coexistence of optical solitons with MI at the same parameter region, and from the potential applicability of optical solitons in context of optical information processing [6, 7].

In principle one expects MI to occur only with coherent beams. If the nonlinear material however exhibits a noninstantaneous response, the observation of MI with incoherent beams is possible, if the phase fluctuations of the beam are faster than the response time of the material [5, 8–11]. MI of incoherent beams up to now has been studied with an approach regarding an isotropic material response. Assuming such a spatially isotropic material response, the filamentation transversal to the propagation direction, is also expected to occur isotropically. In case of anisotropic media, such as photorefractive crystals, commonly used in experiment, also an anisotropic nonlinear response must be expected. And indeed, for coherent beams it is observed, that dependent on either the strength of the nonlinearity or the propagation distance the uniform beam breaks up first into stripes and only later on full two dimensional beam filaments develop [2]. As an one dimensional isotropic approach cannot cover this anisotropy induced aspects, we study in this paper fully

two dimensional modulation instability of incoherent beams including effects caused by material anisotropy. The dependence of the onset of modulation instability on coherence is investigated both experimentally and numerically in photorefractive media .

Secondary modulation instability in experiment

The light source for the experiment is a Nd:YAG cw-laser at 532 nm. To create a partially incoherent beam a rotating diffuser is placed between two lenses in 4f arrangement. The degree of spatial coherence is controlled with the diffuser position on the $z-$axis. The collimated beam propagates through a SBN:61 crystal (5mm x 5mm x 23mm) to which an external electric field is applied along the crystal's $\hat{c}$-axis. The beam is extraordinarily polarized and thus experiences a nonlinear change of refractive index depending on the external field and on the total light intensity. The dark current density of the crystal is controlled with a white light background illumination. The intensity distribution at the crystal's backplane is recorded with a CCD- camera, while the input intensity is measured with a photodiode. As equivalent to the spatial coherence length l_c the average FWHM of the speckles at the crystal's frontplane is taken. The diffuser rotates much faster than the material's response time τ, which is in the order of a second for the crystal in use [12].

The intensity output was monitored at fixed coherence length l_c, while the nonlinearity of the SBN crystal was increased by raising the externally applied voltage U_{ext} in increments of 100 Volts. Images of the beam profile were recorded at every voltage step after 2 minutes, permitting for transients to relax out. The applied voltage was restricted to maximum values of 1.5 kV to avoid damage of the crystal. Experiments were performed in the same manner at different coherence lengths ($l_c = 280$ μm - 9 μm). During all measurements input intensity as well as background illumination were kept constant. In figure 1a experimental images of developing MI are shown. Rows depict system states at equal nonlinearity, while columns show pictures at equal coherence properties. At a fixed coherence length l_c (e.g. the $l_c = 280$ μm column) at first a stripe pattern, perpendicularly to the $\hat{c}$-axis, develops, followed by the formation of spot like filaments at higher voltages. From the images one can conclude that as well formation of (1+1)D stripes as the decay of stripes in (2+1)D filaments occurs at higher nonlinearities, if the coherence length is decreased.

Numerical simulation of incoherent MI in anisotropic media

We also numerically simulated the propagation of an incoherent light beam in an anisotropic photorefractive medium. A light beam propagating through a photorefractive medium in z-direction can be described in paraxial approximation by the equation

$$2ik_0 n_e \frac{\partial}{\partial z} A + \nabla_\perp^2 A = -k_0^2 n_e^4 r_{33} \frac{\partial \varphi}{\partial x} A \,, \tag{1}$$

where $\nabla_\perp = \partial_x^2 + \partial_y^2$, k_0 is the vacuum wavenumber of the light beam, n_e is the refractive index of the (unperturbed) medium and r_{33} is the effective element of the electro-optical tensor. φ is the electric space charge potential inside the medium. In agreement with the experiments we used, $k_0 = 2\pi/532$ nm, $n_e = 2.3$ and $r_{33} = 180$ pm/V. A is the envelope of the electric field of the light beam. To cover for the incoherence of the light beam the coherent density model is used, which states that incoherent light can be described as a superposition of many coherent, yet mutually incoherent components, propagating in slightly different directions. We thus express the light beam

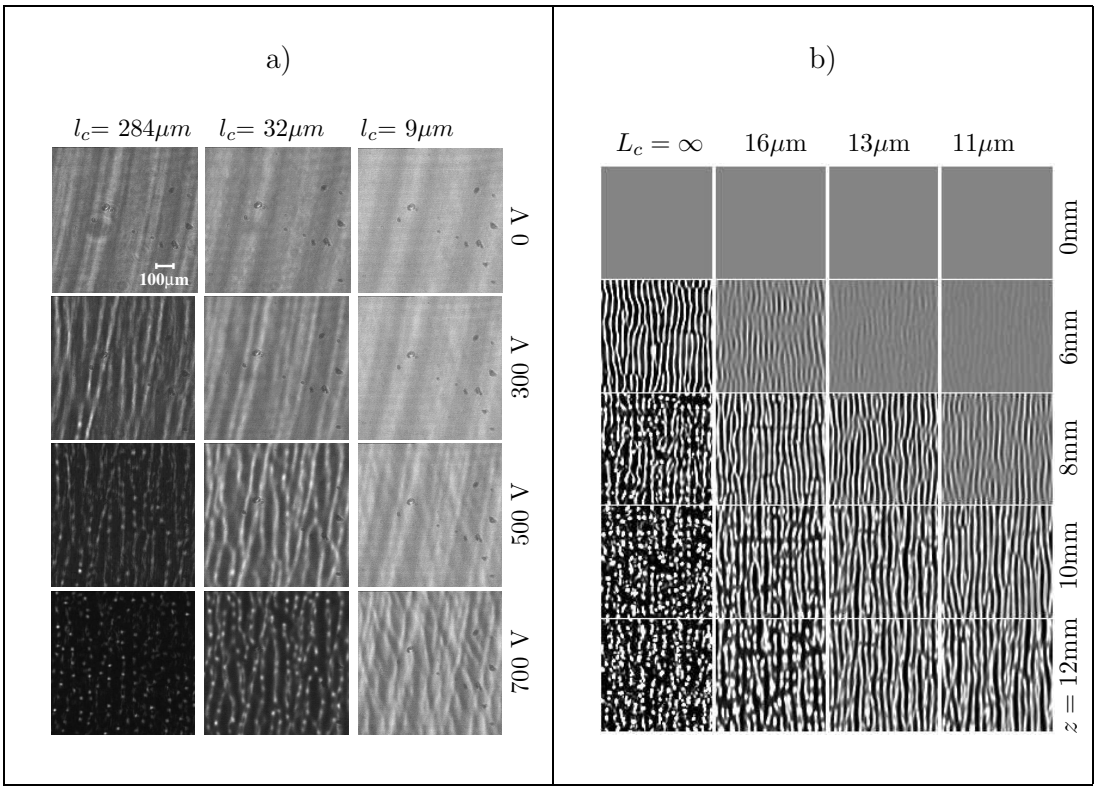

Fig. 1. a) Experimental images of MI. Images in rows show equal nonlinearity. Images in columns show equal coherence length. b) Numerical simulations: Rows depict equal propagation distance. Columns depict equal coherence properties.

at the input face of the medium as:

$$A(x,y,0) = \sum_{k_x,k_y} P(x,y)\exp(i(k_x x + k_y y))$$
$$\frac{l_c}{\sqrt{\pi}}\sqrt{\exp(-(k_x^2+k_y^2)l_c^2/2)}\exp(i\gamma_{k_x,k_y}(t))\,, \tag{2}$$

where $|P(x,y)|^2$ is the intensity profile at the input face, k_x and k_y stand for the slight tilting of the different components, l_c is the coherence length of the light and $\gamma_{k_x,k_y}(t)$ are uncorrelated random phase factors, thus making the single components mutually incoherent.

Photorefractive crystals are known to be well described by the Kukhtarev equations, which yield, using a few well justified approximations, the following differential equation for the space charge potential [13]:

$$\nabla_\perp^2\varphi + \nabla_\perp \ln(1+I)\nabla_\perp\varphi = E_0\frac{\partial}{\partial x}\ln(1+I)\,, \tag{3}$$

where E_0 is the external field applied parallel to the crystal's $\hat{c}$-axis and I is the intensity of the light beam, scaled to the dark intensity I_d, describing the excitation of charge carriers into the

conduction band by thermal excitation or background illumination of the crystal.

Figure 1b shows the results of the numerical propagation of light with different degrees of coherence. Each column shows light with a different value of l_c. The leftmost column shows the fully coherent case, i.e. $l_c = \infty$, while for the other columns $l_c = 16$ μm, 13 μm and 11 μm from left to right. The light beam is shown at the input face, after $z = 6$ mm, 8 mm, 10 mm and 12 mm of propagation. Note, increasing the propagation distance z in numerics is equivalent to an increase of the external voltage used in experiment if the transverse plane is scaled with $\sqrt{E}$. The pictures show that for all degrees of coherence, MI first breaks the plane wave into stripes oriented perpendicular to the $\hat{c} - axis$. In the coherent case, these stripes then break into filaments. If the degree of coherence of the light is decreased, however, the breaking of the stripes can be suppressed. For $l_c = 16\mu$m one can see that extent of the filaments in the vertical direction is much longer than in the case of the fully coherent light. Decreasing of the degree of coherence further then leads to a complete stabilization of the stripes. Reducing the degree of coherence even further probably would lead to a complete suppression of MI.

Determination of experimental thresholds

We measure the averaged experimental image contrast $C = \langle (I_{max} - I_{min})/(I_{max} + I_{min}) \rangle$ perpendicular ($C(x)$) and parallel ($C(y)$) to the $\hat{c}$-axis, plotted in figure 2, to determine experimental thresholds for the onset of (1+1)D MI and (2+1)D MI.

The curves in the graph are guides for the eye, which connect measurement points at fixed coherence lengths l_c referred to in the legend of figure 2a.

Due to the formation of (1+1)D stripes a rise of contrast in $C(x)$ is observed. Instead of a saturation level, expected if only (1+1)D MI was involved, a decrease in $C(x)$ is observed after a maximum value. Simultaneously with the decrease of $C(x)$ a rise of $C(y)$ sets in. We assume that decrease in $C(x)$ as well as rise of $C(y)$ result from the onset of (2+1)D MI. As experimental thresholds for MI we define a rise of the contrast function C(x) for (1+1)D MI and C(y) for (2+1)D MI above a level of $(1 - 1/e) = 63\%$ times the maximum of contrast [14]. As exceptions of this behaviour $l_c = 9$ μm and 19 μm have to be considered, here a absolute maximum of contrast in $C(y)$ and in $C(x)$ is not reached below 1.5 kV. Thus a correct experimental threshold cannot be derived for these coherence lengths. The values derived can however be considered as a lower limit for the experimental thresholds. Also at these small coherence length the characteristics of the structure formed by MI changes to a zig-zag kind of pattern. Compare to the numerical result at low coherence length, which indicates similar beahviour.

In figure 2c experimental thresholds for (1+1)D and (2+1)D MI, derived from the contrast measurements, are plotted. The experimental threshold of (1+1)D MI is denoted by (+), the experimental threshold of (2+1)D MI are indicated by ($*$). At first the values of (1+1)D and (2+1)D MI do not significantly change with decreased coherence length. In this parameter region also both threshold approximatively have a fixed ratio to each other, which can be viewed as indication for the anisotropy of the SBN crystal's nonlinear response. From a coherence length of approximately $l_c = 45$ μm onwards however both experimental thresholds start to alter and a steep increase of thresholds is observed. Likely at this point the influence of incoherent fluctuations pushes the experimental thresholds of MI upwards and here also the fixed relation between thresholds ceases to exist. The experimental thresholds for(2+1)D MI at $l_c = 9$ μm and 19 μm are to be neglected, because the zig-zag kind of pattern forms. Full (2+1)D MI may however exist at higher nonlinear-

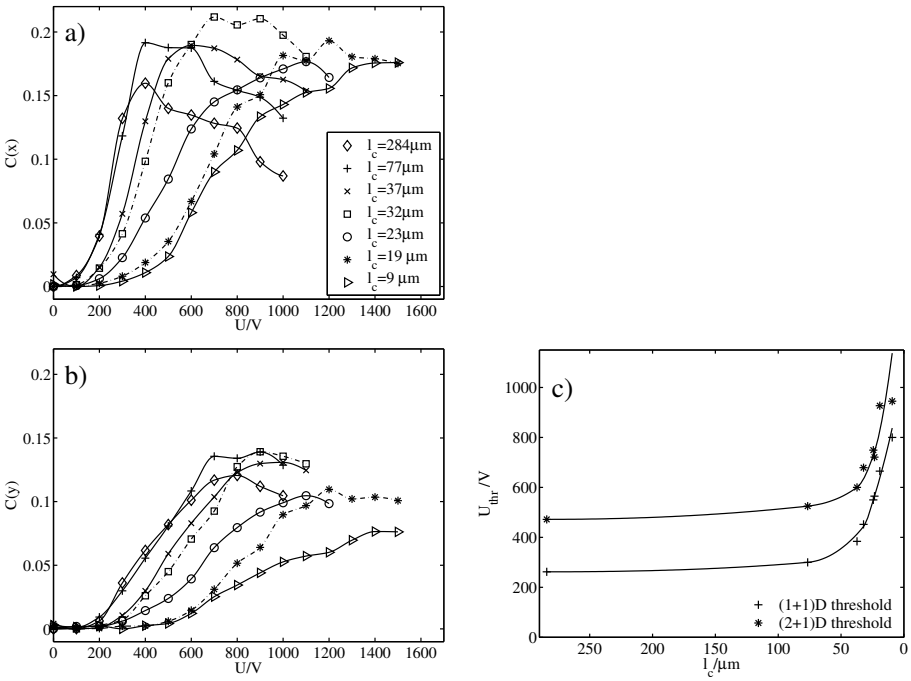

Fig. 2. a) Plot of the average contrast $C(x)$ -parallel to the $\hat{c}$-axis- and b) $C(y)$ over the applied voltage. The legend (a) also applies to (b). c) Plot of first (+) and secondary (*) experimental threshold of MI derived from $C(x)$ and $C(y)$ in dependence on the coherence length. The lines are guides to the eye.

ities.

In conclusion, we found good qualitative agreement of experimental and numerical results and we have determined experimental thresholds for MI. Note, theoretically, thresholds for the onset of nonlinear behaviour are commonly determined using a linear stability anlalysis. Therefore we refrain from determination of theroretical thersholds.

References and Links

1. VI Bespalov and VI Talanov. Filamentary structure of light beams in nonlinear liquids. *JETP Letters-USSR*, 3(12):307, 1966.
2. A. V. Mamaev, M. Saffman, D. Z. Anderson, and A. A. Zozulya. Propagation of light beams in anisotropic nonlinear media: From symmetry breaking to spatial turbulence. *Phys. Rev. A*, 54(1):870, 1996.
3. A. V. Mamaev, M. Saffman, and A. A. Zozulya. Break-up of two-dimensional bright spatial solitons due to transverse modulation instability. *Europhysics Letters*, 35(1):25, 1996.
4. M. Peccianti, C. Conti, and G. Assanto. Optical modulational instability in a nonlocal medium. *Phys. Rev. E*, 68:R025602, 2003.
5. J. Klinger, H. Martin, and Z. Chen. Experiments on induced modulational instability of an incoherent optical beam. *Opt. Lett.*, 26(5):271, 2001.

6. M. Segev, B. Crosignani, A. Yariv, and B. Fischer. Spatial solitons in photorefractive media. *Phys. Rev. Lett.*, 68(7):923–926, 1992.
7. J. Petter, J. Schröder, D. Träger, and C. Denz. Optical control of arrays of photorefractive screening solitons. *Opt. Lett.*, 28(6):438, 2003.
8. M. Soljacic, M. Segev, T. Coskun, D. N. Christodoulides, and A. Vishwanath. Modulation instability of incoherent beams in noninstantaneous nonlinear media. *Phys. Rev. Lett.*, 84:467, 2000.
9. S. M. Sears, M. Soljacic, D. N. Christodoulides, and M. Segev. Pattern formation via symmetry breaking in nonlinear weakly correlated systems. *Phys. Rev. E*, 65:036620, 2002.
10. D. Kip, M. Soljacic, M. Segev, S. M. Sears, and D. N. Christodoulides. (1+1)-dimensional modulation instability of spatially incoherent light. *J. Opt. Soc. Am. B*, 19(3):502, 2002.
11. D. Kip, M. Soljacic, M. Segev, E. Eugenieva, and D. N. Christodoulides. Modulation instability and pattern formation in spatially incoherent light beams. *Science*, 290:495, 2000.
12. K. Buse, A. Gerwens, S. Wevering, and E. Krätzig. Charge-transport parameters of photorefractive strontium-barium niobate crystals doped with cerium. *Josa B*, 15(6):1674, 1998.
13. A. A. Zozulya and D. Z. Anderson. Propagation of an optical beam in a photorefractive medium in the presence of a photogalvanic nonlinearity or an externally applied electric field. *Physical Review A*, 51(2):1520, 1995.
14. B. Gütlich, C. Denz, T. König, K. Motzek, and F. Kaiser submitted to. *Opt. Comm.*